ResearchGate

See discussions, stats, and author profiles for this publication at: https://www.researchgate.net/publication/7245611

Affinity Labeling of the Rabbit 12/15-Lipoxygenase Using Azido Derivatives of Arachidonic Acid †

ARTICLE *in* BIOCHEMISTRY · APRIL 2006

Impact Factor: 3.02 · DOI: 10.1021/bi052152i · Source: PubMed

CITATIONS
14

READS
12

5 AUTHORS, INCLUDING:

Hartmut Kühn
Charité Universitätsmedizin Berlin

363 PUBLICATIONS **9,914** CITATIONS

SEE PROFILE

Igor Ivanov
University of Rostock

63 PUBLICATIONS **636** CITATIONS

SEE PROFILE

Available from: Hartmut Kühn
Retrieved on: 02 February 2016

Affinity Labeling of the Rabbit 12/15-Lipoxygenase Using Azido Derivatives of Arachidonic Acid†

Stepan Romanov,‡,§ Rainer Wiesner,‡ Galina Myagkova,§ Hartmut Kuhn,*,‡ and Igor Ivanov‡,§

Institute of Biochemistry, University Medicine Berlin−Charité, Monbijoustrasse 2, 10117 Berlin, Germany, and Lomonosov State Academy of Fine Chemical Technology, 119571 Moscow, Russian Federation

Received October 21, 2005; Revised Manuscript Received January 20, 2006

ABSTRACT: Lipoxygenases are lipid-peroxidizing enzymes, which have been implicated in the pathogenesis of important diseases. They consist of a single polypeptide chain, which is folded into a two-domain structure. The large catalytic domain contains the putative substrate-binding pocket and the catalytic non-heme iron. To identify structural elements of the rabbit 12/15-lipoxygenase that are involved in enzyme/substrate and/or enzyme/product interaction, we synthesized a set of radioactively labeled lipoxygenase substrates carrying a photoreactive azido group (17-azido-ETE, 18-azido-ETE, 19-azido-ETE) and used these compounds as affinity probes. After photoaffinity labeling, the enzyme was digested proteolytically and modified tryptic cleavage peptides were identified by a combination of radio-HPLC and mass spectral analysis. Following this strategy, we observed covalent linkage of a cleavage peptide that contained Ile593, which has previously been identified as the sequence determinant for the positional specificity. These data are consistent with the previous suggestion that this peptide lines the substrate-binding pocket. Surprisingly, we also observed strong labeling of cleavage peptides originating from the N-terminal β-barrel domain, and our mass spectral data suggested covalent linkage of oxidized affinity probes. Taken together, these results confirm the previous conclusion that Ile593 and surrounding amino acids are constituents of the active site, but they also implicate the N-terminal β-barrel in enzyme/substrate and/or enzyme/product interaction.

Lipoxygenases constitute a heterogeneous family of fatty acid dioxygenases that are widely distributed in plants and animals (*1*, *2*). Completion of the human genome project revealed that there are six functional LOX[1] genes, which encode for six different human isoenzymes (*3*). The biological activity of most mammalian LOX-isoforms is not completely understood, but five LOXs are involved in the biosynthesis of inflammatory leukotrienes (*1*). Other LOX-isozymes have been implicated in cell differentiation (*4*), cancer metastasis (*5*), and atherogenesis (*6*). More recently, involvement of 15-LOX1 in bone development has been suggested (*7*).

The structural biology of the LOX family is not well-developed. For now, the crystal structures of two plant LOX-isoforms [soybean LOX-1 (*8*, *9*) and LOX-3 (*10*)] and one mammalian enzyme/inhibitor complex (*11*) have been reported, and there are additional data sets for various plant LOX−ligand complexes (*12*, *13*). Moreover, a 3D-model for the structure of the human 5-LOX has been worked out (*14*). All LOX-isoforms constitute single polypeptide molecules that are folded into a two-domain structure (*8*−*11*). The large C-terminal catalytic domain of the rabbit 15-LOX-1 comprises about 550 amino acids and is largely helical (*11*). It contains the catalytic non-heme iron, which is buried deeply inside the putative substrate-binding pocket. Its small N-terminal domain involves 110 amino acids and consists of two four-stranded antiparallel β-sheets. It shares a 1.600 Å^2 interface with the catalytic domain (*11*), and the two domains are covalently interconnected by an unstructured stretch (random coil) of amino acids (residues 111−124). The soybean LOX-1, which is composed of 839 amino acids, does also fold into a two-domain structure (*8*, *9*). The two subunits share a 2.600 Å^2 contact plane, and the interdomain interface constitutes a solvent-filled crevice (*9*). Detailed evaluation of the corresponding X-ray coordinates (comparison of the *B*-value pattern) suggested that the overall structures of the two domains are rather stable but that the N-terminal β-barrel domain may move as stable unit relative to the catalytic subunit (*9*). Recent investigations into the solution structure of the rabbit 15-LOXs (*15*) are supportive for this hypothesis, but similar experiments on the soybean LOX did not reveal any indications for significant interdomain movement (*16*).

† Financial support was provided by the Humboldt Foundation (RUS-111557), DAAD (A/03/01297), and the European Commission (FP6, LSHM-CT-2004-0050333).

* To whom correspondence should be addressed: Dr. Hartmut Kuhn, Institute of Biochemistry, University Medicine Berlin−Charite, Humboldt University, Monbijoustr. 2, 10117 Berlin, F. R. Germany. Tel, +49-30-450528040; fax, +49-30-450528905; e-mail, hartmut.kuehn@charite.de.

‡ University Medicine Berlinz−Charité.

§ Lomonosov State Academy of Fine Chemical Technology.

[1] Abbreviations: RP-HPLC, reverse-phase high-performance liquid chromatography; SP-HPLC, straight-phase high-performance liquid chromatography; LOXs, lipoxygenases; GC/MS, gas chromatography/mass spectrometry; AA, (5*Z*,8*Z*,11*Z*,14*Z*)-eicosa-5,8,11,14-tetraenoic (arachidonic) acid; [$^3H_8$]-17-azido-ETE, [5,6,8,9,11,12,14,15-$^3H_8$]-(5*Z*,8*Z*,11*Z*,14*Z*)-17-azidoeicosa-5,8,11,14-tetraenoic acid; [$^3H_8$]-18-azido-ETE, [5,6,8,9,11,12,14,15-$^3H_8$]-(5*Z*,8*Z*,11*Z*,14*Z*)-18-azidoeicosa-5,8,11,14-tetraenoic acid; [$^3H_8$]-19-azido-ETE, [5,6,8,9,11,12,14,15-$^3H_8$]-(5*Z*,8*Z*,11*Z*,14*Z*)-19-azidoeicosa-5,8,11,14-tetraenoic acid.

10.1021/bi052152i CCC: $33.50 © 2006 American Chemical Society
Published on Web 02/28/2006

Despite this structural information, the binding fatty acid derivatives at the active site of mammalian LOXs have not been investigated in detail. There is no crystal structure of a mammalian LOX−substrate complex, and affinity-labeling studies have not been carried out. In addition, the functional relevance of the N-terminal β-barrel domain is far from understood. Limited proteolysis studies on the soybean LOX-1 led to the formation of a truncated LOX-form that lacked the N-terminal β-barrel (*17*). This mini-LOX was catalytically active and exhibited an impaired affinity for linoleic acid (K_M of 11.2 μM for native and 24.2 μM for mini-LOX). On the other hand, V_{max} of linoleic acid oxygenation was augmented (363 s^{-1} for mini-LOX vs 55 s^{-1} for the native enzyme). These data suggested that the N-terminal β-barrel domain may not be essential for the catalytic cycle but might be involved in substrate binding and/or product dissociation. Gene technical truncation of the N-terminal β-barrel domain of the rabbit 15-LOX (*18*) led to the formation of a mini-LOX, which exhibited a similar substrate affinity as the native enzyme (7.0 μM for mini-LOX vs 11.4 μM for the native enzyme) but a lower catalytic activity (V_{max} of 9.9 s^{-1} for the native enzyme vs 1.6 s^{-1} for the mini-LOX).

To explore which structural elements of the rabbit 12/15-LOX directly interact with fatty acid substrates and/or hydroperoxy fatty acid activators, we initiated experiments using a specific affinity probe. For this purpose, we synthesized (*19*, *20*) a set of radioactively labeled arachidonic acid derivatives, which carry a photoreactive azido group at different carbon atoms of the fatty acid backbone (17-azido-ETE, 18-azido-ETE, 19-azido-ETE) and incubated these compounds with the purified rabbit 15-LOX. After tryptic digestion, we identified labeled cleavage peptides and assigned them to the 3D-structure of the enzyme. Among labeled cleavage fragments, we identified a 3.5 kDa peptide (amino acids 571−599) that contained the amino acid I593, which has previously identified as sequence determinant for the positional specificity of the rabbit enzyme (*21*). In the 3D-structure, I593 acid is localized in immediate proximity to L589 and Q590, which constitute sequence determinants for the positional specificity of the human 15-LOX2 (*22*), and thus, this region of the primary structure appears to line the substrate-binding cleft of the enzyme. Surprisingly, we also observed strong labeling of β-barrel domain peptides. These data suggest that the N-terminal β-barrel domain, which does not contribute to the active site according to the X-ray coordinates, appears to interact with substrate fatty acids and/or their oxygenation products.

MATERIALS AND METHODS

Chemicals. The chemicals used were from the following sources: sodium borohydride from Serva (Heidelberg, Germany); nitrosomethyl urea, bis[trimethylsilyl]trifluoroacetamide (BSTFA), and trypsin from Sigma (Deisenhofen, Germany); 10% Pd/$CaCO_3$ (catalyst for hydrogenation) from Aldrich (Taufkirchen, Germany). All solvents were of HPLC grade and purchased from Baker (Deventer, The Netherlands). The azido fatty acids used in this study were synthesized as reported before (*19*, *20*).

Preparation of the Native Rabbit 15-LOX. The native reticulocyte-type 15-LOX was prepared from the stroma-free hemolysis supernatant of a reticulocyte-rich blood cell suspension by sequential ammonium sulfate precipitation, hydrophobic interaction chromatography, and anion exchange chromatography on a preparative Mono-Q column (Pharmacia, Uppsala, Sweden). The final enzyme preparation was electrophoretically pure (<95%) and exhibited a linoleic acid turnover rate of about 20 s^{-1}. Protein concentration of the 15-LOX preparations was determined with the Roti-Quant kit (Carl Roth GmbH, Karlsruhe, Germany).

Recombinant Enzyme Expression, Purification, and N-Terminal Truncation. The recombinant wild-type 15-LOX and the C-truncated mutant were expressed in *Escherichia coli* as His-tagged fusion proteins and purified to near homogeneity by affinity chromatography on a Ni−agarose column (*18*). For deletion of the N-terminal β-barrel domain, a *Sal*I restriction site was introduced in front of Cys115 by site-directed mutagenesis. This procedure led to an N-terminal truncation mutant that lacked the first 114 amino acids (*18*).

Spectrophotometric Measurements of LOX Activity. The oxygenation kinetics of the fatty acid derivatives were assayed spectrophotometrically measuring the increase in absorbance at 235 nm (formation of conjugated dienes) in the substrate concentration range of 10−200 μM at room temperature. The assay mixture consisted of 0.1 M phosphate buffer (pH 7.4) containing various concentrations of fatty acid substrate as sodium salts. Before addition of the enzyme (2−15 μg), the assay mixture was sonicated for 30 s to achieve homogeneous dispersion of the substrate.

Product Preparation and Analysis. For analysis of the oxygenation products formed by LOX-species, aliquots of purified enzyme preparations were incubated with azido fatty acids (in 10−150 μM range of final substrate concentration) at room temperature for 15−20 min. The hydroperoxy fatty acids formed were reduced to the corresponding hydroxy derivatives with sodium borohydride. The lipophilic products were extracted with ethyl acetate, and the solvent was evaporated. The residue was reconstituted in 0.5 mL of methanol, and aliquots were analyzed by RP-HPLC.

HPLC analysis of the fatty acid derivatives was performed with a Shimadzu LC-6A liquid chromatograph connected to an Agilent 1100 diode array detector. Separation of the fatty acid derivatives was performed on a Nucleosil C-18 column (Macherey-Nagel, Düren, Germany; 250 mm × 4 mm, 5 μm particle size) and a guard-column (30 mm × 4 mm, 5 mm particle size, same vendor). The solvent system was a mixture of methanol/water/acetic acid (85:15:0.1, by volume), and a flow rate of 1 mL/min was used. The absorbance at 235 nm was recorded. SP-HPLC was performed on a Nucleosil 100-7 column (Macherey-Nagel, Düren, Germany; 250 mm × 4 mm, 5 μm particle size) with the solvent system hexane/2-propanol/acetic acid (98.5:1.5:0.1, by volume) and a flow rate of 1 mL/min.

For gas chromatography/mass spectroscopy (GC/MS) analysis, the azido hydroxy fatty acids (10 μg) were prepared by RP- and/or SP-HPLC, methylated with diazomethane, and hydrogenated using 10% Pd/$CaCO_3$ (Merck, Germany) as a catalyst. This procedure did also reduce azido group. Amino and hydroxy groups were silylated with bis[trimethylsilyl]-trifluoroacetamide in dry pyridine. GC/MS was carried out on a Shimadzu GC-MS QP-2000 system equipped with a fused silica column SPB 1 (10 m × 0.25 mm, coating

thickness 0.25 μm). An injector temperature of 270 °C, an ion source temperature of 180 °C, and electron energy of 70 eV were adjusted. The derivatized fatty acids were eluted with the following temperature program: isothermically at 180 °C for 2 min and then from 180 to 290 °C at a rate of 5 °C/min.

Affinity Labeling of the Enzyme. For routine experiments, 1.5 nmol of the pure rabbit 15-LOX was incubated in 0.5 mL of 0.1 M phosphate buffer (pH 7.4) with either radioactive affinity probe (75 nmol, 1.5 mCi/mmol) or nonlabeled analogues on ice, and the mixture was irradiated for 2 min with UV-light (254 nm). Then, 1 mL of ice-cold acetone was added, and the sample was kept at −20 °C for 2 h. The protein precipitate was spun down (2 min at 10 000 rpm), and the pellet was washed three times to remove excess probe: first wash, 1 mL of MeOH/$CHCl_3$ mixture (1:2, by volume); second wash, 1 mL of MeOH/H_2O mixture (4:1, by volume); and third wash, 1 mL of acetone. The solvent was evaporated in a vacuum centrifuge, and the protein pellet was stored at −80 °C for further workup.

Proteolytic Digestion and Characterization of Cleavage Peptides. The protein pellet was dispersed by sonication in 1 mL of NH_4HCO_3 buffer (pH 8.3) using a tip-sonifier (30 s, 50 W). The derivatized protein was trypsinated (trypsin/15-LOX ratio 1:50, w/w) overnight at 37 °C, and the cleavage peptides were analyzed by RP-HPLC. HPLC analysis of the cleavage peptides mixture was performed on a Shimadzu LC-6A liquid chromatograph connected to a SPD-6AV UV−vis detector (215 nm) using a Discovery BIO Wide Pore C18 column (Supelco, Sigma-Aldrich, Germany; 150 mm × 4.6 mm, 5 μm particle size), which was connected to a guard-column (20 mm × 4 mm, 5 μm particle size; same vendor). Cleavage peptides were eluted using a segmented gradient of acetonitrile (CH_3CN) in water containing 0.1% trifluoroacetic acid: first segment, 5 min isocratic elution at 2% CH_3CN; second segment, linear increase in CH_3CN concentration from 2% to 45% in 55 min; third segment, linear increase of CH_3CN concentration from 45% to 100% in 10 min; and fourth segment, 10 min isocratic elution at 100% CH_3CN. A flow rate of 1 mL/min was adjusted. Under these conditions, the tryptic cleavage peptides of the unmodified 15-LOX were eluted within the first 60 min. The column effluent was fractionated (1 min fractions), and the different fractions were subjected to liquid scintillation counting using a Wallac 1410 counter (Pharmacia, Finland).

Mass Spectrometric Analysis of the Cleavage Peptides. The solvents of the HPLC-fractions (1 mL each) were evaporated under vacuum, and the residue was reconstituted in 10 μL of a mixture containing CH_3CN/H_2O/TFA (50:50:0.1, by volume). The mass spectra were recorded with a MALDI-TOF mass spectrometer (Voyager-DE PRO, Applied Biosystems, Framingham, MA) using α-cyano-4-hydroxycinnamic acid as matrix. The spectra were obtained in the linear mode averaging 200 laser slots with an acceleration voltage of 20 kV, a 93% grid voltage, and 100−200 ns delay. An acquisition range of *m*/*z* 500−14 000 was adjusted. For analysis of mass spectrometric data, a GPMAW program (General Protein Mass Analysis for Windows) was used. The accuracy of our mass spectral analysis was ±1 Da.

Structural Modeling of Enzyme/Substrate Complex. The 15-LOX/substrate complex (Figure 4) was constructed on the basis of the crystal structure (*11*) of the rabbit reticulocyte 15-LOX (PDB entry 1LOX). The residues, which were not defined in the crystal structure (601−602, 210−211, 177−187), were inserted in silico using the molecular visualization program VMD (*23*), and energy was minimized using the molecular simulation program NAMD (*24*).

RESULTS

Substrate Behavior of Aliphatic Azido Derivatives of Arachidonic Acid. Although affinity-labeling with modified substrates is a frequently used method to investigate the mechanism of enzyme−substrate interactions, this strategy has not been applied in LOX research. We synthesized a set of radioactively labeled arachidonic acid derivatives, which carry a photoreactive azido group at different carbon atoms of the fatty acid backbone (azido-ETE). To test whether these azido fatty acids are properly bound at the active site of the rabbit 12/15-LOX, we first investigated their oxygenation behavior. Spectrophotometric measurements (Figure 1A) indicated the formation of conjugated dienes during the incubation of the pure rabbit 15-LOX with the affinity probes, and the reaction rates were comparable to that of arachidonic acid. More detailed kinetic analysis (K_M of 10.9 μM) suggested high-affinity binding of 19-azido-ETE (*19*). This value is in the same range of the corresponding constants for other polyenoic fatty acids (*25*). The V_{max} for 19-azido-ETE conversion (20 s^{-1} with this particular enzyme preparation) was also comparable with the corresponding value for arachidonic acid oxygenation. These data indicated that after a 3 s incubation period the entire affinity probe added to a typical labeling experiment was converted to the corresponding hydroperoxide.

If 19-azido-ETE is bound at the active site like arachidonic acid, the pattern of reaction products should be similar. SP-HPLC analysis of 19-azido-ETE oxygenation products revealed the formation of one major conjugated diene with an absorbance maximum at 235 nm (Figure 1B), and the UV-spectral properties suggested a *Z*,*E*-conjugated diene chromophore (inset). The minor product eluting with a retention time of 9.9 min did also contain a conjugated diene chromophore, but the blue-shifted absorbance maximum (231 nm) suggested *E*,*E*-double bond geometry.

The electron impact mass spectrum of the hydrogenated derivative of the major oxygenation product (Figure 1C) was characterized by ions at *m*/*z* 343 originating from α-cleavage (inset) and *m*/*z* 170 [$CH(OTMS)CH_2CH_2CH_2CH(NHTMS)$-$CH_3$−90]. These data suggest that lipoxygenation of the affinity probe had occurred at C-15. More detailed analysis of the mass spectral data are given in the legend to Figure 1C. Analysis (HPLC and mass spectrometry) of the oxygenation products of 17-azido- and 18-azido-ETE isomers revealed the formation of a more heterogeneous product mixture. Although LC−MS analysis suggested that the major reaction products derived from C-15 oxygenation, HPLC data indicated a low degree of reaction specificity. In fact, several product isomers containing a conjugated diene chromophore were detected in SP-HPLC, but their detailed structure was not completely clarified.

Affinity Labeling of 15-LOX Using 19-Azido-EET. Since 19-azido-ETE exhibited major similarities with arachidonic acid in the above-described experiments, this probe was

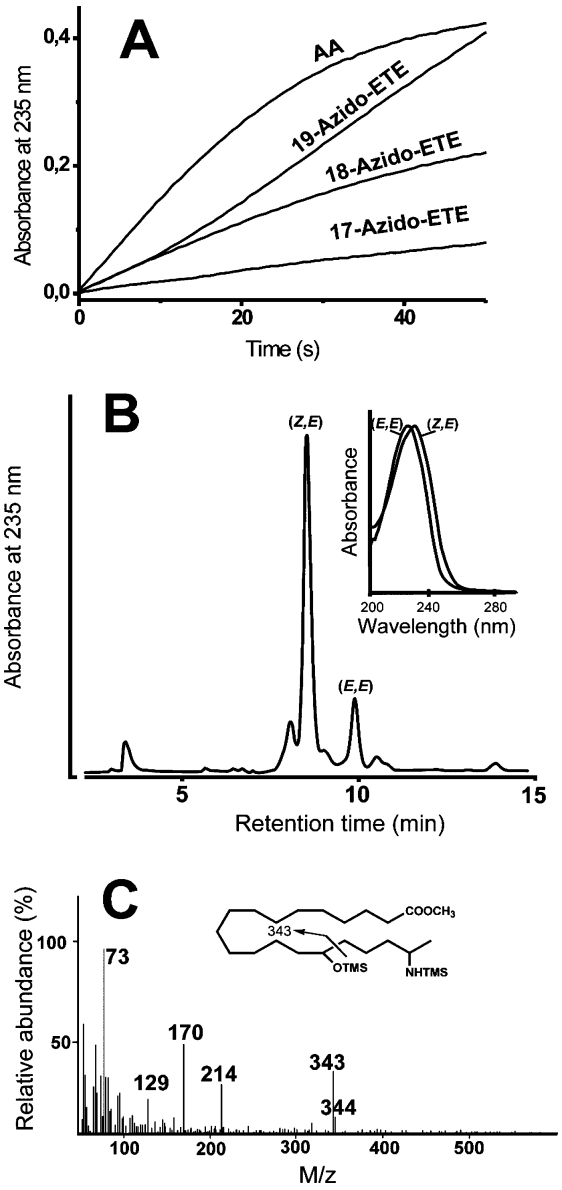

FIGURE 1: Substrate behavior of various affinity probes. (A) Activity assays: the pure rabbit 15-LOX (4 μg/mL) was incubated in phosphate buffer, pH 7.4, in the presence of 25 μM of the various fatty acids. The absorbance at 235 nm was recorded. (B) Product analysis: the pure rabbit 15-LOX (4 μg/mL) was incubated with of 19-azido-ETE. After 10 min, the sample was acidified and the lipids were extracted. The conjugated dienes were prepared by RP-HPLC and further analyzed by SP-HPLC on a Nucleosil 100-7 column (250 mm $\times$ 4 mm, 5 μm particle size) using a mixture of hexane/2-propanol/acetic acid (98.5:1.5:0.1, by volume) as solvent at a flow rate of 1 mL/min. Inset: UV spectra of the major reaction products. (C) Mass spectral analysis of the major oxygenation product: the major conjugated diene was prepared by SP-HPLC and methylated (incubation with diazomethane), and the double bonds were hydrogenated. This treatment reduced the azido group to the corresponding amine. The hydroxy groups were subsequently silylated with bis(trimethylsilyl)trifluoroacetamide in dry pyridine. Mass spectral analyses were performed as described in Materials and Methods. The ions at *m/z* 214 and 129 may represent [$(CH_2)_{11}$-$COOCH_3$] and [$CH_2CH_2CHOTMS$], respectively.

selected for affinity labeling. Because of the unspecific product patterns, 17-azido- and 18-azido-ETE were not used for these experiments. In preliminary experiments, we first optimized the labeling conditions and started with a molar enzyme/probe ratio of 1:1. Unfortunately, under these conditions, we did not observe significant labeling of the

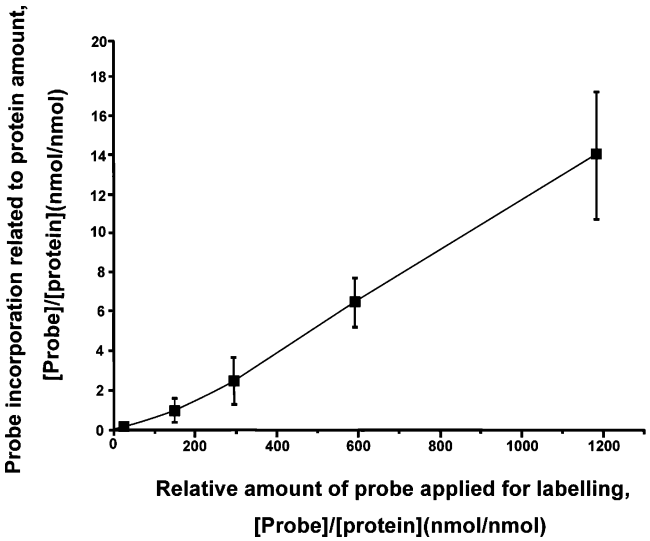

FIGURE 2: Affinity labeling of rabbit 15-LOX1 using 19-azido-ETE as probe. Pure rabbit 12/15-LOX (1.5 nmol) was incubated in 0.5 mL of 0.1 M phosphate buffer (pH 7.4) with various amounts of radioactive 19-azido-ETE on ice. The mixture was irradiated for 2 min at 254 nm, and 1 mL of ice-cold acetone was added to precipitate the protein. The precipitate was spun down and washed extensively to remove the excess of radioactive probe (see Materials and Methods). Then the precipitate was dispersed in phosphate buffer using a tip sonifier, and aliquots were subjected to liquid scintillation counting.

enzyme protein. Next, we gradually increased the probe concentration up to an enzyme/probe ratio of 1:1000 and detected an increase in labeling efficiency (Figure 2). To avoid excess of unspecific labeling, we selected an enzyme/probe ratio of 1:50 for subsequent labeling experiments. When 1.5 nmol of 12/15-LOX was labeled with a 50-fold molar excess of radioactive 19-azido-ETE, we found that about 0.30 nmol of labeled affinity probe was covalently linked to the enzyme protein. These data suggested that in average 0.2 mol of 19-azido-ETE was attached to each mole of 15-LOX protein. In other words, one out of five protein molecules was labeled under these experimental conditions.

Tryptic Cleavage of Affinity-Labeled 15-LOX. For more detailed information on the sites of covalent attachment of the affinity probe, the labeled protein was precipitated, dispersed in a volatile buffer, and cleaved with trypsin. The cleavage peptides were then separated by RP-HPLC, and absorbance of the column effluent at 215 nm was monitored. Fractions of 1 mL were collected, and radioactivity was counted. From Figure 3A, one can see that the affinity probe (no 15-LOX) eluted as a single peak with a retention time of 73.5 min. The UV-chromatogram of tryptic cleavage peptides obtained from labeled 15-LOX is shown in Figure 3B. We observe that the majority of the cleavage peptides were eluted with a retention time between 25 and 45 min. In contrast, the bulk of radioactivity was eluted between 67 and 73 min (Figure 3C). We stress that similar chromatograms were obtained when the native 15-LOX (unlabeled) was digested (data not shown). Thus, evaluation of the UV-profiles (differential chromatograms) did not allow identification of labeled cleavage peptides. Two major conclusions may be drawn from the outcome of our labeling experiments: (i) The majority of the cleavage peptides has not been modified during the labeling procedure. (ii) The labeled

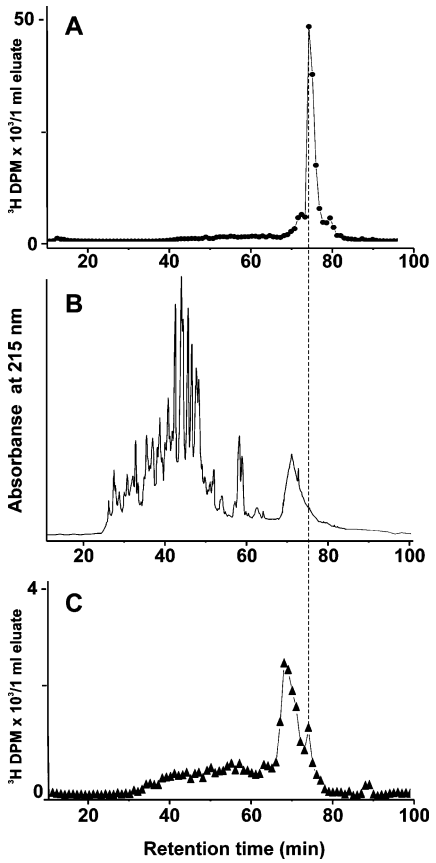

FIGURE 3: RP-HPLC analysis of tryptic cleavage peptides of native and affinity-labeled 12/15-LOX. The rabbit 12/15-LOX (100 μg) was affinity-labeled with [$^3H_8$]-19-azido-ETE (see Materials and Methods). After tryptic cleavage, the resulting peptides were analyzed by RP-HPLC on a Discovery BIO Wide Pore C18 column (Supelco, Sigma-Aldrich, Germany, 150 mm $\times$ 4.6 mm, 5 μm particle size) with a guard-column (20 mm $\times$ 4 mm, 5 mm particle size, same vendor) using a segmented gradient of acetonitrile in water (see Materials and Methods). The absorbance at 215 nm and the radioactivity were simultaneously recorded. (A) HPLC analysis of the affinity probe; (B) tryptic cleavage peptides from affinity-labeled 15-LOX1 recording the absorbance at 215 nm; (C) radioactivity profile of the tryptic cleavage peptides from affinity-labeled 15-LOX1.

cleavage peptides were eluted in HPLC between 67 and 73 min.

MALDI-TOF Analysis of the Modified Cleavage Peptides. To identify the cleavage peptides linked to the affinity probe, labeling experiments were performed with nonradioactive 19-azido-ETE. The affinity probe was omitted in corresponding control incubations. Then the two samples were taken through the same experimental protocol (incubation, precipitation, washing, tryptic digest, and HPLC), and the fractions eluting in HPLC between 67 and 73 min were collected and further analyzed by MALDI-TOF mass spectrometry. Applying this strategy, we obtained two databases of mass ions (labeled peptides and control peptides), which were subsequently subtracted from each other. The resulting "differential database" was then searched for ions, the masses of which corresponded to cleavage peptides that were covalently linked to either oxygenated or nonoxygenated 19-azido-ETE. In the first round of screening, we focused on masses with a cleavage peptide/probe ratio of 1:1. Since our affinity probe constitutes a LOX substrate, which binds at the active site with high affinity, we first looked for cleavage peptide lining the putative substrate-binding pocket. Searching our differential database, we identified a mass ion with *m*/*z* 3560, which may have originated from covalent linkage of 19-azido-ETE to the cleavage peptide D571-R599. This mass ion was clearly absent in the control mass database (no affinity probe). Evaluating the amino acid sequence of this cleavage peptide (Table 1), we found that it contained the amino acid I593, which has been identified as a sequence determinant for the positional specificity of the rabbit 15-LOX (*21*). Moreover, this peptide contains L589 and Q590, which act as sequence determinants for the positional specificity of the human 15-LOX2 (*22*). Structural modeling indicated that at least the C-terminal part of this peptide lines the substrate-binding pocket and the amino acids L589 (not shown) and Q590−I593 (Figure 4A) are located in close proximity to C-19 of the fatty acid backbone that carries the photoreactive azido group. We note that the N-terminal part of this cleavage peptide is located at the protein surface and, thus, may also be susceptible to unspecific labeling.

More detailed search of our differential mass database revealed labeling of five additional tryptic cleavage peptides, which were all located in the N-terminal β-barrel domain (Table 1). These data were quite surprising since the X-ray coordinates do not provide evidence for a possible interaction of the β-barrel domain with the putative substrate-binding cleft. However, our affinity labeling data indicated that several cleavage peptides of this structural element were covalently modified (Figure 4B). Interestingly, all of these labeled cleavage peptides contained oxygenated 19-azido-ETE. We stress that these data do not exclude the possibility that the N-terminal β-barrel domain may also be capable of interacting with nonoxidized affinity probe since under our experimental conditions the probe is completely oxidized during the first 3 s of the incubation period. Thus, our results implicate the β-barrel domain in enzyme/substrate and/or enzyme−product interaction.

Impact of the N-Terminal β-Barrel Domain on Suicidal Inactivation. Hydroperoxy fatty acids have multiple functions for LOXs. They convert catalytically silent ferrous LOX species to their active ferric forms (*26*), but they also inactivate LOX-isoforms irreversibly (*27*). Moreover, they constitute suitable LOX substrates, which are converted via multiple catalytic activities of the enzymes to secondary reaction products (*28*, *19*, *30*). To test whether the N-terminal β-barrel domain might be involved in peroxide-dependent suicidal inactivation, we prepared the β-barrel truncation mutant of the rabbit 12/15-LOX (*18*) and compared its kinetic properties with the wild-type enzyme. From Figure 5A, we see that the truncation mutant rapidly loses its catalytic activity. In fact, after about 20 s, we did not see any further increase in absorbance at 235 nm. In contrast, the wild-type enzyme continued to produce conjugated dienes over a longer period of time. These data suggested that the N-terminal β-barrel domain prevents suicidal inactivation. To test the protective effect in more detail, we carried out inactivation studies using 15S-HpETE as inactivator. From Figure 5B, we see that the β-barrel truncation mutant is rapidly inactivated under our experimental conditions. After 20 s of incubation with 2 μM 15S-HpETE, almost 90% of the activity was lost. In contrast, the wild-type enzyme was more resistant to inactivation.

Table 1: Experimental (MALDI-TOF) and Calculated Mass Data for Labeled 15-LOX Peptides[a]

peptide number	amino acid	sequence	mass detected	mass expected	localization (domain)	attached probe
I	2−45	GVYRVCVSTGASIYAGSKNKVELWLVGQHGEVELGSCLRPTRNK	5113.00	5111.89	N-terminal	oxygenated
II	2−68	GVYRVCVSTGASIYA- - -RPTRNKEEEFKVNVSKYLGSLLFVRLRKK	7877.05	7877.24	N-terminal	oxygenated
III	22−50	VELWLVGQHGEVELGSCLRPTRNKEEEFK	3733.10	3733.30	N-terminal	oxygenated
IV	46−72	EEEFKVNVSKYLGSLLFVRLRKKHFLK	3658.68	3659.44	N-terminal	oxygenated
V	73−99	EDAWFCNWISVQALGAAEDKYWFPCYR	3620.04	3618.13	N-terminal	oxygenated
VI	139−171	LYQWGSWKEGLILNVAGSKLTDLPVDERFLEDK	4141.01	4139.82	C-terminal (surface)	nonoxygenated
VII	571−599	DATLETVMATLPNLHQSS**LQ**MS**I**VWQLGK	3560.23	3559.23	C-terminal (active site)	nonoxygenated

[a] The pure rabbit 12/15-LOX (100 μg) was affinity-labeled with a 50-fold molar excess of 19-azido-ETE as described in Materials and Methods. After tryptic cleavage, the fractions containing the modified peptides eluting between 65 and 73 min were prepared by RP-HPLC (see Figure 3) and analyzed by MALDI-TOF mass spectrometry. The sequence determinants for the positional specificity (L, Q, I) in the D571−K599 peptide are labeled in bold. The N-terminal methionine was set amino acid number 1, although it is not present in the final protein (post-translational cleavage).

DISCUSSION

LOXs are single polypeptide enzymes, and the polypeptide chain is folded into a two-domain structure. The large C-terminal domain contains the putative substrate-binding pocket (*9*, *11*), but for the moment, there are no direct experimental data characterizing the topology of enzyme−substrate interaction. Here, we employed an affinity labeling approach to explore enzyme−substrate interaction and found that two tryptic cleavage peptides of the catalytic domain of the rabbit 12/15-LOX were covalently linked to 19-azido-ETE. One of these peptides (L139−K171) was located at the protein surface, and thus, labeling may be unspecific. The second peptide (D571−R599) contained amino acids which have previously been identified as sequence determinants for the positional specificity of the two LOX-isoforms (*21*, *22*). These mutagenesis results, our labeling data, and the outcome of structural modeling of the enzyme/substrate complex strongly suggest that the D571−R599 cleavage peptide may be considered a part of the substrate-binding pocket. The detailed mechanism of the labeling procedure has not been investigated in this study. It is well-known that UV-irradiation of azido compounds generates labile nitrene intermediates (*31*), which subsequently react with amino groups, oxygen moieties, or even with hydrophobic residues in the immediate vicinity of their formation at a diffusion-controlled reaction rate. Unfortunately, we were unable to identify the covalently modified amino acids experimentally. However, to suggest candidate residues for covalent linkage, we modeled the enzyme−arachidonic acid complex (Figure 4A) and searched the immediate surrounding of carbon-19 for susceptible amino acids. We found that the site chain atoms of L589 (not shown), M591, and I593 are located in close proximity to the photoreactive azido group. Other candidate amino acids (Q590, S592, Q596), which are also localized in this region of the primary structure (Figure 4A), are unlikely to be modified because of their large distances (>6 Å) to the reactive azido group.

The strong labeling of cleavage peptides of the N-terminal β-barrel domain was rather surprising since this structural element has not been implicated in enzyme/substrate and/or enzyme/product interactions. In general, the function of the N-terminal β-barrel domain is still a matter of discussion. The high degree of conservation of the two-domain structure in most LOXs suggests the catalytic importance of this structural element, but for now, its functionality is far from clear. Because of its structural similarity to the β-barrel domain of human lipases (*32*), the N-terminal domains of mammalian LOXs have been implicated in membrane binding. Indeed, site-directed mutagenesis of surface-exposed tryptophanes in the N-terminal domain impaired membrane binding of the human 5-LOX (*33*). For the rabbit 12/15-LOX gene, technical truncation of the β-barrel domain also induced impairment of membrane binding, but site-directed mutagenesis studies suggested that surface-exposed amino acids in both domains are involved in membrane binding (*18*). For the soybean LOX1, proteolytic cleavage of the N-terminal β-barrel domain augmented its membrane binding capacity (*17*), which contrasts the results obtained with the two mammalian LOXs (5-LOX and 12/15-LOX). To precisely define the role of the N-terminal β-barrel domain in membrane binding, truncation and mutagenesis studies on other LOX-isoforms should be carried out and such experiments are underway in our laboratory.

In addition to a possible role in membrane binding, a regulatory activity of the β-barrel domain for the catalytic reaction has been suggested (*17*, *18*). Gene technical truncation of the rabbit 12/15-LOX impaired the catalytic efficiency of the enzyme (*18*), whereas limited proteolysis of the soybean LOX1 augmented oxygenase activity (*17*). Moreover, suicidal inactivation of LOXs appears to be regulated by the β-barrel domain. It has been reported previously and was confirmed in this study that the N-terminal truncation mutant of the rabbit 12/15-LOX undergoes more rapid suicidal inactivation during arachidonic acid oxygenation when compared with the wild-type enzyme. The N-terminal truncation mutant completely lost its activity within the first 20 s of arachidonic acid oxygenation (Figure 5A), and similar results were obtained when the enzyme was incubated in the presence of 2 μM 15-HpETE (Figure 5B). In contrast, the complete recombinant enzyme was much more stable (Figure 5). These data, together with our finding that β-barrel domain cleavage peptides were covalently linked to oxygenated derivatives of 19-azido-ETE, strongly suggest that this domain may be involved in peroxide binding and, thus, appears to be of dual regulatory importance for catalytic efficiency. It may impact both peroxide-dependent enzyme activation and suicidal inactivation.

Another catalytic subprocess, which might be impacted by the β-barrel domain, is substrate binding. Kinetic studies on the N-terminal-truncated mini-LOXs from soybeans indicated an impaired affinity for substrate fatty acids (K_M of 11.2 μM for native and 24.2 μM for mini-LOX),

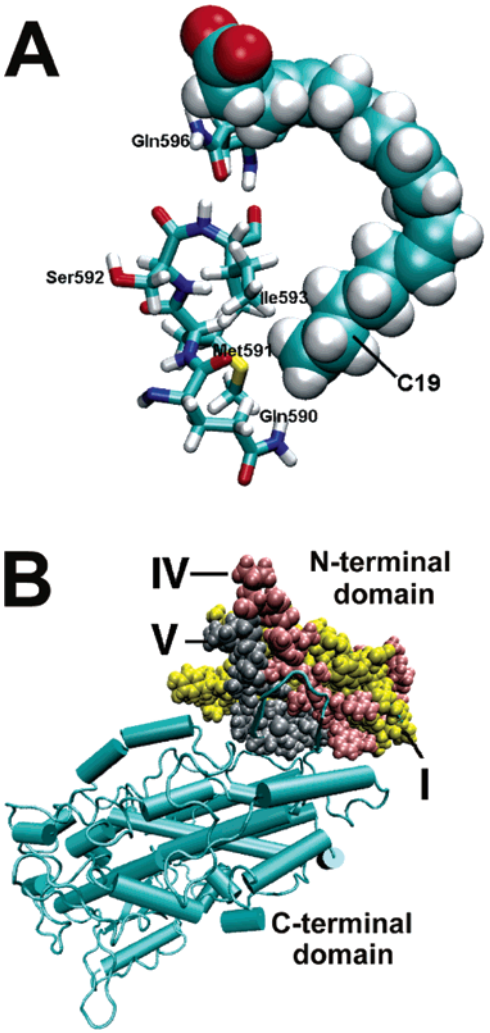

FIGURE 4: Affinity-modified tryptic cleavage peptides. The rabbit 12/15-LOX was affinity-labeled with nonradioactive 19-azido-ETE as described in the legend of Table 1, and the most prominent modified cleavage peptides are shown. The X-ray coordinates (*11*) of the rabbit 12/15-LOX were used to construct the structural model of the enzyme/substrate complex (PDB entry 1LOX). The residues, which were not defined in the crystal structure (601−602, 210−211, 177−187), were inserted in silico using the molecular visualization program VMD (*23*), and energy was minimized using the molecular simulation program NAMD (*24*). Modeling of the enzyme substrate complex has been reported before (*21*). (A) Affinity labeling of the active site peptide (peptide VII in Table 1) containing the sequence determinant for the positional specificity I593. Potential candidate amino acids for covalent linkage are indicated (see text). (B) The modified tryptic cleavage peptide I, IV, and V, which together comprise more the 90% of the N-terminal β-barrel domain, are shown in different colors.

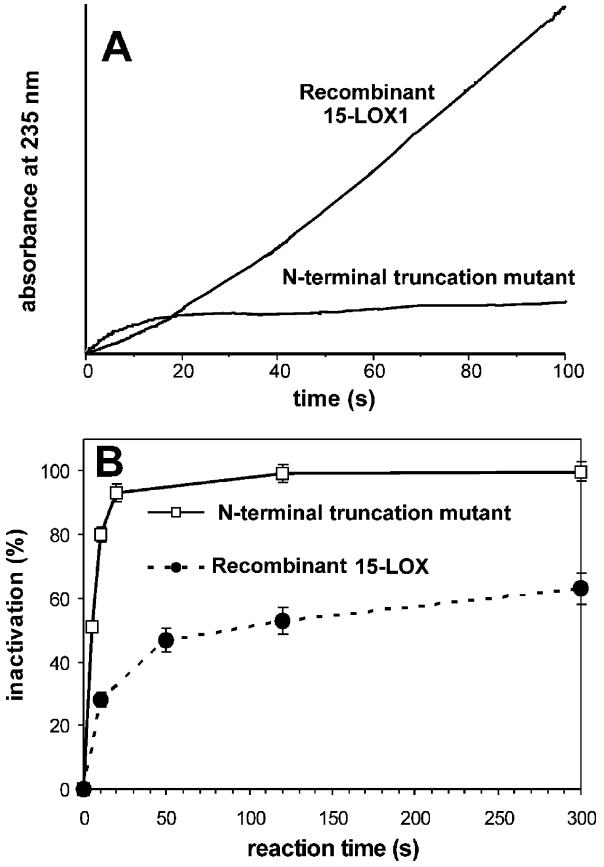

FIGURE 5: Impact of β-barrel domain on the reaction kinetics of the recombinant rabbit 12/15-LOX. (A) Progress curves of arachidonic acid oxygenation. The wild-type recombinant 12/15-LOX and its β-barrel truncation mutant were expressed as His-tag fusion proteins and purified as described in Materials and Methods. Aliquots (1 μg of the wild-type enzyme and 8 μg of the truncation mutant) were used to assay the arachidonic acid oxygenase activity (100 μM) with a Shimadzu UV2100 spectrophotometer (reaction volume 1 mL). (B) Time course of 12/15-LOX inactivation by 15*S*-HpETE: the recombinant 15-LOX (30 μg/mL) and the β-barrel truncation mutant (50 μg/mL) were incubated with 15*S*-HpETE (2 μM) in 0.1 M phosphate buffer, pH 7.4. At the times indicated, aliquots were taken off and the residual linoleic acid oxygenase activity was assayed. Each data point represents the mean of triplicate measurements.

suggesting a role of the N-terminal domain in substrate acquisition (*17*). Our finding of strong affinity labeling of cleavage peptides of the N-terminal domain is consistent with this hypothesis, and the fact that we only detected linkage-oxidized 19-azido-ETE does not argue against this hypothesis. Oxygenated polyenoic fatty acids are true LOX substrates, which are converted to double (*28*, *34*) or triple oxygenation products (*29*), to epoxy leukotrienes (*30*, *35*), and hepoxilins (*36*). These reactions require proper substrate alignment at the active site, and the N-terminal β-barrel domain may help to achieve this goal. Moreover, our failure to detect linkage of the nonoxidized affinity probe may be related to technical problems. Under our experimental conditions, 19-azido-ETE is rapidly oxygenated during the incubation period, and after about 3 s, almost the entire amount of affinity probe was oxidized. Although we attempted to keep the preincubation period (before irradiation) as short as possible, it could not be completely eliminated. Another potential problem, which should be taken into account when interpreting our labeling data, is the possibility that the oxygenated affinity probe exhibits an altered photoreactivity. Although such functional interaction of the two groups is rather unlikely because of their large physical distance (azido group at C19 and peroxy group at C15), it cannot be completely excluded. To avoid these problems, labeling studies should be carried out under anaerobic conditions. Unfortunately, complete anaerobiosis is difficult to achieve in our experimental setup since repeated evacuation of the sample and flushing with argon inactivates the enzyme. The specificity of the labeling process has not been studied in detail, and the surface exposure of the β-barrel domain may contribute to its heavy labeling. However, there are many unlabeled surface-exposed cleavage peptides of the

catalytic domain, suggesting a certain degree of specificity in β-domain labeling.

Despite these methodological difficulties, the strong labeling of the N-terminal β-barrel domain suggested a role of this structural element in enzyme/substrate and/or enzyme/product interactions. Since both processes are important for the efficiency of the catalytic cycle, the β-barrel domain of LOX appears to be of regulatory importance. Moreover, affinity labeling of an active site peptide that contains a sequence determinant for the positional specificity confirmed the previous hypothesis that the U-shaped cavity identified in the crystal structure constitutes the substrate-binding pocket.

ACKNOWLEDGMENT

The technical assistance of Ms. P. Kunert (MALDI-TOF analysis) is acknowledged.

SUPPORTING INFORMATION AVAILABLE

Peptide sequence of the rabbit reticulocyte 15-LOX and tables of mass ions detected in the HPLC fractions prepared from the native and affinity-labelled 15-LOX. This material is available free of charge via the Internet at http://pubs.acs.org.

REFERENCES

1. Brash, A. R. (1999) Lipoxygenases: occurrence, functions, catalysis, and acquisition of substrate, *J. Biol. Chem. 274*, 23679−23682.
2. Grechkin, A. (1998) Recent developments in biochemistry of the plant lipoxygenase pathway, *Prog. Lipid Res. 37*, 317−352.
3. Funk, C. D., Chen, X. S., Johnson, E. N., and Zhao, L. (2002) Lipoxygenase genes and their targeted disruption, *Prostaglandins Other Lipid Mediators 68−69*, 303−312.
4. van Leyen, K., Duvoisin, R. M., Engelhardt, H., and Wiedmann, M. (1998) A function for lipoxygenase in programmed organelle degradation, *Nature 395*, 392−395.
5. Kim, E., Rundhaug, J. E., Benavides, F., Yang, P., Newman, R. A., and Fischer, S. M. (2005) An antitumorigenic role for murine 8S-lipoxygenase in skin carcinogenesis, *Oncogene 224*, 1174−1187.
6. Huo, Y., Zhao, L., Hyman, M. C., Shashkin, P., Harry, B. L., Burcin, T., Forlow, B., Stark, M. A., Smith, D. F., Clarke, S.; Srinivasan, S., Hedrick, C.C., Praticò, D., Witztum, J. L., Nadler, J. L., Funk, C. D., and Ley, K. (2004) Critical role of macrophage 12/15-lipoxygenase for atherosclerosis in apolipoprotein E-deficient mice, *Circulation 110*, 2024−2031.
7. Klein, R. F., Allard, J., Avnur, Z., Nikolcheva, T., Rotstein, D., Carlos, A. S., Shea, M., Waters, R. V., Belknap, J. K., Peltz, G., and Orwoll, E. S. (2004) Regulation of bone mass in mice by the lipoxygenase gene Alox15, *Science 303*, 229−232.
8. Boyington, J. C., Gaffney, B. J., and Amzel, L. M. (1993) The three-dimensional structure of an arachidonic acid 15-lipoxygenase, *Science 260*, 1482−1486.
9. Minor, W., Steczko, J., Stec, B., Otwinowski, Z., Bolin, J. T., Walter, R., and Axelrod, B. (1996) Crystal structure of soybean lipoxygenase L-1 at 1.4 Å resolution, *Biochemistry 35*, 10687−10701.
10. Skrzypczak-Jankun, E., Amzel, L. M., Kroa, B. A., and Funk, M. O., Jr. (1997) Structure of soybean lipoxygenase L3 and a comparison with its L1 isoenzyme, *Proteins 29*, 15−31.
11. Gillmor, S. A., Villasenor, A., Fletterick, R., Sigal, E., and Browner, M. F. (1997) The structure of mammalian 15-lipoxygenase reveals similarity to the lipases and the determinants of substrate specificity, *Nat. Struct. Biol. 4*, 1003−1009.
12. Skrzypeczak-Jankun, E., Bross, R. A., Carroll, R. T., Dunham, W. R., and Funk, M. O. (2001) Three-dimensional structure of a purple lipoxygenase, *J. Am. Chem. Soc. 123*, 10814−10820.
13. Borbulevych, O. Y., Jankun, J., Selman, S. H., and Skrzypeczak-Jankun, E. (2004) Lipoxygenase interactions with natural flavonoid, quercitin, reveal a complex with protocatechuic acid in its X-ray structure at 2.2 Å resolution, *Proteins 54*, 13−19.
14. Hemak, J., Gale, D., and Brock, T. G. (2002) Structural characterization of the catalytic domain of the human 5-lipoxygenase enzyme, *J. Mol. Model. 8*, 102−112.
15. Hammel, M., Walther, M., Prassl, R., and Kuhn, H. (2004) Structural flexibility of the N-terminal β-barrel domain of 15-lipoxygenase-1 probed by small-angle X-ray scattering. Functional consequences for activity regulation and membrane binding, *J. Mol. Biol. 343*, 917−929.
16. Dainese, E., Sabatucci, A., van Zadelhoff, G., Angelucci, C. B., Vachette, P., Veldink, G. A., Agro, A. F., and Maccarrone, M. (2005) Structural stability of soybean lipoxygenase-1 in solution as probed by small-angle X-ray scattering, *J. Mol. Biol. 349*, 143−152.
17. Maccarrone, M., Salucci, M. L., van Zadelhoff, G., Malatesta, F., Veldink, G., Vliegenthart, J. F. G., and Finazzi-Agro, A. (2001) Tryptic digestion of soybean lipoxygenase-1 generates a 60 kDa fragment with improved activity and membrane binding ability, *Biochemistry 40*, 6819−6827.
18. Walther, M., Anton, M., Wiedmann, M., Fletterick, R., and Kuhn, H. (2002) The N-terminal domain of the reticulocyte-type 15-lipoxygenase is not essential for enzymatic activity but contains determinants for membrane binding, *J. Biol. Chem. 277*, 27360−27366.
19. Romanov, S. G., Ivanov, I. V., Shevchenko, V. P., Nagaev, I. Y., Pushkov, A. A., Myasoedov, N. F., Myagkova, G. I., and Kuhn, H. (2004) Synthesis of (5Z,8Z,11Z,14Z)-18- and 19-azidoeicosa-5,8,11,14-tetraenoic acids and their (5,6,8,9,11,12,14,15-$^3H_8$]-analogues through a common synthetic route, *Chem. Phys. Lipids 130*, 117−126.
20. Ivanov, I. V., Romanov, S. G., Shevchenko, V. P., Rozhkova, E. A., Maslov, M. A., Groza, N. V., Myasoedov, N. F., Kuhn, H., and Myagkova, G. I. (2003) A convergent synthesis of (17*R*,5*Z*,8*Z*,11*Z*,14*Z*)-17-hydroxyeicosa-5,8,11,14-tetraenoic acid analogues and their tritiated derivatives, *Tetrahedron 59*, 8091−8097.
21. Borngräber, S., Browner, M., Gillmor, S., Gerth, C., Anton, M., Fletterick, R., and Kuhn, H. (1999) Shape and specificity in mammalian 15-lipoxygenase active site. The functional interplay of sequence determinants for the reaction specificity, *J. Biol. Chem. 274*, 37345−37350.
22. Jisaka, M., Kim, R. B., Boeglin, W. E., and Brash, A. R. (2000) Identification of amino acid determinants of the positional specificity of mouse 8S-lipoxygenase and human 15S-lipoxygenase-2, *J. Biol. Chem. 275*, 1287−1293.
23. Humphrey, W., Dalke, A., and Schulten, K. (1996) VMD-visual molecular dynamics, *J. Mol. Graphics 14*, 33−38.
24. Kale, L., Skeel, R., Bhandarkar, M., Brunner, R., Gursoy, R., Krawetz, N., Phillips, J., Shinozaki, J., Varadarajan, K., and Schulten, K. (1999) NAMD2: greater scalability for parallel molecular dynamics, *J. Comput. Phys. 151*, 283−312.
25. Ludwig, P., Holzhütter, H. G., Colosimo, A., Silvestrini, C., Schewe, T., and Rapoport, S. M. (1987) A kinetic model for lipoxygenases based on experimental data with the lipoxygenase of reticulocytes, *Eur. J. Biochem. 168*, 325−337.
26. de Groot, J. J., Veldink, G. A., Vliegenthart, J. F., Boldingh, J., Wever, R., and van Gelder, B. F. (1975) Demonstration by EPR spectroscopy of the functional role of iron in soybean lipoxygenase-1, *Biochim. Biophys. Acta 377*, 71−79.
27. Yamamoto, S., Suzuki, H., and Ueda, N. (1997) Arachidonate 12-lipoxygenases, *Prog. Lipid Res. 36*, 23−41.
28. van Os, C. P., Rijke-Schilder, G. P., Van Halbeek, H., Verhagen, J., and Vliegenthart, J. F. (1981) Double dioxygenation of arachidonic acid by soybean lipoxygenase-1. Kinetics and regio-stereo specificities of the reaction steps, *Biochim. Biophys. Acta 663*, 177−193.
29. Kühn, H., Wiesner, R., Alder, L., Fitzsimmons, B. J., Rokach, J., and Brash, A. R. (1987) Formation of lipoxin B by the pure reticulocyte lipoxygenase, *Eur. J. Biochem. 169*, 5923−5601.
30. Maas, R. L., and Brash, A. R. (1983) Evidence for a lipoxygenase mechanism in the biosynthesis of epoxide and dihydroxy leukotrienes from 15(S)-hydroperoxyicosatetraenoic acid by human platelets and porcine leukocytes, *Proc. Natl. Acad. Sci. U.S.A. 80*, 2884−2888.
31. Bayley, H. (1983) *Photogenerated Reagents in Biochemistry and Molecular Biology*, Vol.12, Elsevier, New York.
32. Winkler, F. K., D'Arcy, A., and Hunziker, W. (1990) Structure of the human pancreatic lipase, *Nature 343*, 771−774.

33. Kulkarni, S., Das, S., Funk, C. D., Murray, D., and Cho, W. (2001) Molecular basis of the specific subcellular localization of the C-2-like domain of 5-lipoxygenase, *J. Biol. Chem. 277*, 13167−13174.
34. Schwarz, K., Borngräber, S., Anton, M., and Kuhn, H. (1998) Probing the substrate alignment at the active site of 15-lipoxygenases by targeted substrate modification and site-directed mutagenesis. Evidence for an inverse substrate orientation, *Biochemistry 37*, 15327−15335.
35. Shimizu, T., Radmark, O., and Samuelsson, B. (1984) Enzyme with dual lipoxygenase activities catalyzes leukotriene A4 synthesis from arachidonic acidl, *Proc. Natl. Acad. Sci. U.S.A. 81*, 689−693.
36. Nigam, S., Patabhiraman, S., Ciccoli, R., Ishdorj, G., Schwarz, K., Petrucev, B., Kühn, H., and Haeggström, J. Z. (2004) The rat leukocyte-type 12-lipoxygenase exhibits an intrinsic hepoxilin A3 synthase activity, *J. Biol. Chem. 279*, 29023−29030.
37. Wiesner, R., Suzuki, H., Walther, M., Yamamoto, S., and Kuhn, H. (2003) Suicidal inactivation of the rabbit 15-lipoxygenase by 15S-HpETE is paralleled by covalent modification of active site peptides, *Free Radical Biol. Med. 34*, 304−315.

BI052152I